ISSN(Print): 1225-7672 / ISSN(Online): 2287-822X
DOI https://doi.org/10.11001/jksww.2017.31.5.397

Sonoelectrodeposition of RuO_2 electrodes for high chlorine evolution efficiencies

초음파 전기증착법을 활용한 고효율 염소 발생용 루테늄 옥사이드 전극

Tran Le Luu[1]·Choonsoo Kim[2]·Jeyong Yoon[2*]
트란 루 레·김춘수·윤제용

[1]*Department of Mechatronics & Sensor Systems Technology, Vietnamese German University, Le Lai Street, Hoa Phu Ward, Thu Dau Mot City, Binh Duong Province, Viet Nam*
[2]*School of Chemical and Biological Engineering, College of Engineering, Institute of Chemical Process, Asian Institute for Energy, Environment & Sustainability (AIEES), Seoul National University (SNU), Gwanak-gu, Daehak-dong, Seoul 151-742, Korea*
[1]베트남 독일 대학교 메카트로닉스-센서 시스템 학과
[2]서울대학교 화학생물공학부 화학공정 신기술 연구소 & 아시아에너지환경지속가능발전 연구소

ABSTRACT

A dimensionally stable anode based on the RuO_2 electrocatalyst is an important electrode for generating chlorine. The RuO_2 is well-known as an electrode material with high electrocatalytic performance and stability. In this study, sonoelectrodeposition is proposed to synthesize the RuO_2 electrodes. The electrode obtained by this novel process shows better electrocatalytic properties and stability for generating chlorine compared to the conventional one. The high roughness and outer surface area of the RuO_2 electrode from a new fabrication process leads to increase in the chlorine generation rate. This enhanced performance is attributed to the accelerated mass transport rate of the chloride ions from electrolyte to electrode surface. In addition, the electrode with sonodeposition method showed higher stability than the conventional one, which might be explained by the mass coverage enhancement. The effect of sonodeposition time was also investigated, and the electrode with longer deposition time showed higher electrocatalytic performance and stability.

Key words: Chlorine evolution, DSA, Electrocatalyst, RuO2, Sonoelectrodeposition

주제어: 전기화학촉매, 초음파 전기증착법, 루테늄 옥사이드, 염소 발생, 염소발생 전극

1. Introduction

The chlor-alkali industry produces annually around 70 million tons of chlorine in the world, which is one of the most widely used electrochemical technologies. The chlor-alkali process is closely linked to energy and is the second largest consumer product in the electrolytic industry of about 240 billion kWh annually (Srinivasan et al., 2006). The Ruthenium oxide(RuO_2) is a well-known electrode material for its excellent electrocatalytic features as a Dimensionally Stable Anode (DSA) (Luu et al., 2015[a]; Trasatti, 1984; Luu et al, 2015[b]). Roughly, 10-15% of the annual production of Ru is used for the preparation of DSA-type electrodes (Srinivasan et al., 2006).

The RuO_2 electrode is environmentally benign because it reduces the cost, time, and energy consumption and increases the chlorine evolution efficiency as well as its stability

Received 25 July 2017, revised 28 September 2017, accepted 11 October 2017
* Corresponding author: Jeyong Yoon (E-mail: jeyong@snu.ac.kr)

(Katerina et al, 2009). Various methods of synthesizing RuO_2 electrodes have been developed such as sol–gel (Panic et al., 2005), thermal decomposition (Burrows et al., 1978), polyol (Terezo et al., 2002), Adams fusion (Ribeiro et al., 2008), reactive sputtering (Chou et al., 2013), and chemical vapor deposition (Han et al., 2010).

In these methods, the desired catalyst loading can be achieved by several coating applications and calcination steps. Especially, the high temperature vapor-phase processes in reactive or chemical vapor deposition are expensive, and they are limited by their low yield. The electrodeposition method has been proven to be simple, versatile, one-step, film thickness controllable, and cost effective for electrode preparation (Vukovic et al., 1989; Metikos-Hukovic et al., 2006; Hu et al., 2009; Jowa et al., 2007; Tsuji et al., 2011; Burke et al., 1976). The charge transfer and the diffusion of supersaturated ions on the electrode surface, which are major mechanisms of crystal formation in electrodeposition, have been determined by this method (Macherzynskia et al., 2013).

Electrodeposition of RuO_2 based electrodes proceeds through wet chemical precipitation induced by a negative electrode-generating base (Zhitomirsky et al., 1997; Zheng et al., 2008; Zheng et al., 2008; Trieu et al., 2012). As the outer surface is increased, the chlorine over electro potential decreases, and an electro potential reduction in noble RuO_2 can be achieved by the electrodeposition method.

The electrodeposition route for the preparation of the RuO_2 electrode is related to a local cathodic reaction to increase the pH near the electrode surface. The main cathodic reaction to produce OH^- is initiated from the decomposition of water under hydrogen evolution as follows (Zheng et al., 2008; Trieu et al., 2012):

$$O_2 + 2H_2O + 4e- \leftrightarrow 4OH^- \quad (1)$$

$$2H_2O + 2e- \leftrightarrow H_2 + 2OH^- \quad (2)$$

The above reactions consume H_2O, generate OH^-, and then react with Ru ions to form Ru oxide. Hydroxide, or peroxide colloidal particles deposit on cathodic substrates. Ruthenium hydroxide and peroxide deposits can be converted into RuO_2 by thermal treatment. The assumed reactions are represented as follows:

$$Ru^{3+} + OH^- \rightarrow RuO_x(OH)_y \rightarrow RuO_2 \quad (3)$$

In addition, the cathodic decomposition of water competes with the cathodic electrodeposition of the Ru metal:

$$Ru^{4+} + 4e^- \rightarrow Ru^o \quad (4)$$

In recent decades, the use of sonoelectrodeposition has increased rapidly in the production of various nanomaterials (Garcia et al., 2010[a]; Garcia et al., 2010[b]; Hyde et al., 2002; Walker et al., 1997; Mallik et al., 2011; Floaate et al., 2002; Garcia et al., 2002; Saez et al., 2004; Zheng et al., 2008; Lecina et al., 2012; Niu et al., 2012; Pollet et al., 2008; Pollet et al., 2011). It has been shown that the effect of high intensity sonication in electrochemical processes leads to both chemical and physical effects. Sonication decreases the thickness of the diffusion layer which consequently increases the limiting current. The increased limiting current affects the cavitation, micro- and macro-streaming, electrolyte concentration on the electrode surface, and the reaction rate (Garcia et al., 2010[a]; Garcia et al. 2010[b]; Hyde et al. 2002; Walker et al., 1997).

In this study, the cathodic sonoelectrochemical deposition method is proposed for RuO_2 synthesis. The properties of the electrodes synthesized by the sonoelectrodeposition method are compared with conventional ones synthesized by mechanical stirring electrodeposition.

2. Experimental

2.1 Electrode preparation

RuO_2 nanoparticles were deposited onto commercial Ti substrates by cathodic electrodeposition under sonication or mechanical stirring followed by calcination (Burke et al., 1976; (Macherzynskia et al., 2013; Zhitomirsky et al., 1997; Zheng et al., 2008). Ti foils (dimensions, 30 × 20 × 0.25 mm, purity 99.7%, Aldrich-Sigma, USA) were used as the substrate materials. The contaminants of the foil were removed by degreasing in acetone, and then, it was etched in boiling concentrated HCl at 86°C for 1 h to produce a gray surface

with uniform roughness. A Pt electrode (Samsung DSA, Korea) was used as the counter electrode.

The electrochemical bath was prepared by dissolving 5 mM $RuCl_3$ and 20 mM $NaNO_3$ as the supporting electrolyte (99.9 %, Aldrich) in deionized water at room temperature (25˚C). Cathodic deposition was performed at a constant current density of 50 mA/cm^2 controlled by a power source (Unicorn Tech, Korea) with ultrasonic treatment at 20 kHz (Branson, USA) or mechanical agitation at 200 rpm for different deposition times. Next, the electrode was calcined at 450˚C for 1 hr to allow the removal and formation of the functional metal oxide. The backside of the electrode is covered with epoxy to prevent exposure to the electrolyte.

2.2 Microstructure characterization

The amount of RuO_2 nanoparticles deposited on the electrode surface was measured by the weight difference between the electrodes before and after the electrodeposition using a balance (Ohaus E02140, USA; Zhitomirsky et al., 1997).

Microstructures on the electrode surfaces were characterized with a field emission scanning electron microscope (FE-SEM, JSM-6701F, JEOL Co., Japan) and a transmission electron microscope (TEM, JEOL 2000EXII, Japan). The TEM samples were prepared by scraping off the coating using a sharp knife and dispersing the powders in isopropyl alcohol. High resolution X-ray diffraction patterns were obtained to study the crystal structure of the RuO_2 electrodes (Bruker-AXS, Germany).

2.3 Chlorine evolution and electrochemical measurement

Chlorine was evolved by electrolysis in a two-electrode system with the following conditions: an acidic NaCl solution (0.1 M & pH 6) and a current density of 16.7 mA/cm^2. The aqueous active chlorine concentration was determined by the DPD (N, N-diethyl-p-phenylenediamine) colorimetric method (Klug et al., 2001; Jeong et al., 2009; Ardizzone et al., 1990). The experiment was repeated in triplicated, and the average value with standard deviation was reported.

The electrochemical characterizations of the RuO_2 electrodes with cyclic voltammetry (CV) and linear sweep voltammetry (LSV) measurements were carried out in a conventional single compartment cell with three electrodes using a computer-controlled potentiostat (PARSTAT 2273A, Princeton Applied Research, USA) (Jeong et al., 2009). The volume of the electrolyte solution in the cell was 150 mL. RuO_2/Ti, Pt (Samsung Chemicals, Korea), and Ag/AgCl (in saturated KCl) were used as the working electrode (anode), the counter electrode (cathode), and the reference electrode, respectively.

The CV was measured in a 0.5 M H_2SO_4 solution as the electrolyte with the potential ranging between 0-1 V and the scan rate varying from 5-320 mV/s. The voltammetric charge q obtained by integration of the voltammetric curve is a measurement for the size of electrochemically active surface area, which is accessible by the electrolyte.

The inner and outer surface areas were identified by plotting and extrapolating the voltammetric charges according to infinitely low (0) and fast (∞) scan rates, which was reported elsewhere (see more in the supporting information). The pseudo-capacitive reaction, which consists of coupled redox transitions involving proton exchange with the solution at a broad reversible peak around 0.6 V vs. Ag/AgCl, can be described as (APHA et al., 2005):

$$RuO_x(OH)_y + zH^+ + ze^- \rightarrow RuO_{x-z}(OH)_{y+z} \quad (1)$$

LSV measurements were done in an electrolyte containing 5 M NaCl + 0.01 M HCl (pH 2) which is a favorable condition for chlorine evolution (Terezo et al., 2002). The stability of the prepared RuO_2 electrodes was examined using the accelerated stability test (AST) with a considerably higher current density, and an electrolyte solution that is more dilute than those usually used in industrial electrochemical conditions. It provides information on the electrode stability and lifetime (via the electrode potential - time dependence at a constant current density) (Ribeiro et al., 2004; Panic et al., 1999; Aromaa et al., 2006). The experiments were performed galvanostatically at a current density of 1 A/cm^2 in a solution of 0.5 M NaCl, pH 2 at room temperature (25˚C). The potential of RuO_2 electrode was recorded during electrolysis.

3. Results and discussion

3.1 Chlorine evolution properties of RuO_2 electrode by sonoelectrodeposition method

As shown in Fig. 1 (a), the efficiency of the chlorine evolution at Sono-10' produced by sonoelectrodeposition increases to 17.1% compared with Convention-15' produced by conventional stirring electrodeposition.

The chlorine evolution efficiency increases up to 17.1% in the case of the sonoelectrodeposition RuO_2 electrode (171 mg/L) compared to the one made by the conventional stirring electrodeposition (146 mg/L) which was fabricated with the same deposition time of 15 min. Moreover, the chlorine concentration of the RuO_2 electrode produced by sonoelectrodeposition after 10 min is also higher than that prepared conventionally for 15 min.

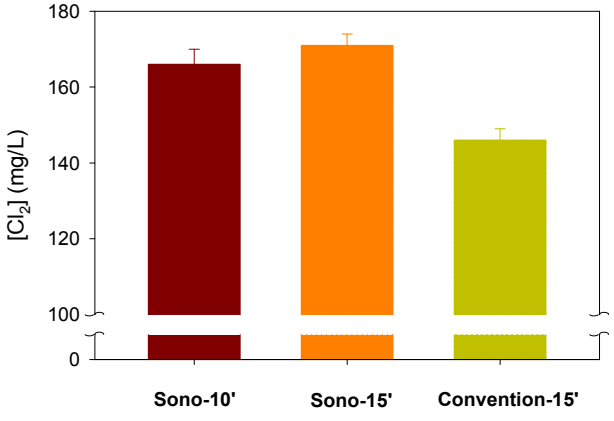

(a)

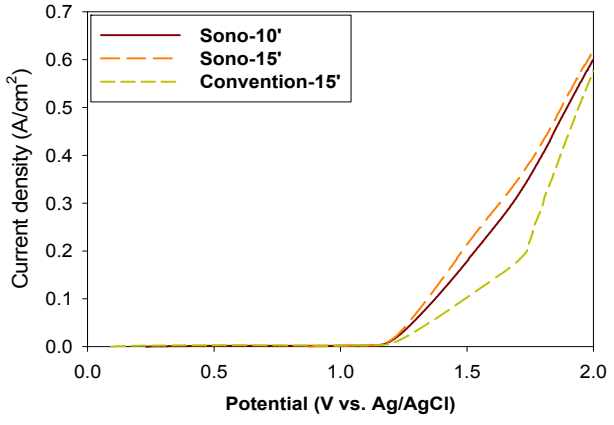

(b)

Fig. 1. Chlorine concentrations (a) and LSV (b) of the RuO_2 electrodes prepared by sonoelectrodeposition and conventional stirring electrodeposition. Sono-x' and convention-x': where x indicates the deposition time (min). (Experimental conditions: (a) 0.1 M NaCl, pH 6, 10 min; (b) 5 M NaCl, pH 2).

As shown in Fig 1 (a), the increases in sonoelectrodeposition time induced higher chlorine evolution performance. Also, the higher current density in LSV (Fig 1. (b)) was observed at the electrode fabricated with longer sonoelectrodeposition time, which supports the result in Fig 1 (a). The current density of each method begins to increase steadily above 1.2 V, which indicates that chlorine generation reaction occurred above 1.2 V. The current densities extracted from the linear sweep voltammograms in the region of chlorine evolution is higher in the electrodes made by sonoelectrodeposition than in the ones produced by conventional stirring electrodeposition. The efficiency of chlorine generation is related to the active surface area, which contributes to the electrochemical reaction.

Clearly, sonoelectrodeposition has a positive role on improving the electrocatalytic performances of RuO_2 electrodes for chlorine evolution compared to the conventional method.

3.2 Surface characterization

Fig. 2 shows the SEM (a) and TEM images (b) of the RuO_2 surfaces made by sonoelectrodeposition and conventional deposition. As shown in Fig. 2 (a), the morphologies of these electrodes show different morphology. The electrode made by sonoelectrodeposition has higher roughness compared to the conventional method. The electrode made by sonochemical deposition contains various structures including big hemispheres, fine grains, and mushroom-like structures, while just a few pebble-like small spheres are deposited with the conventional method. This high roughness with sonoelectrochemical method could enhance the mass transport of chloride ions from electrolyte to the substrate, which is expected to be the main reason for increased electrocatalytic performance with sonoelectrochemical method in section 3.1.

As the sonoelectrodeposition time increases, the roughness and surface coverage increase, and the uniformity of RuO_2 increases. It means that the sonication strongly affects the

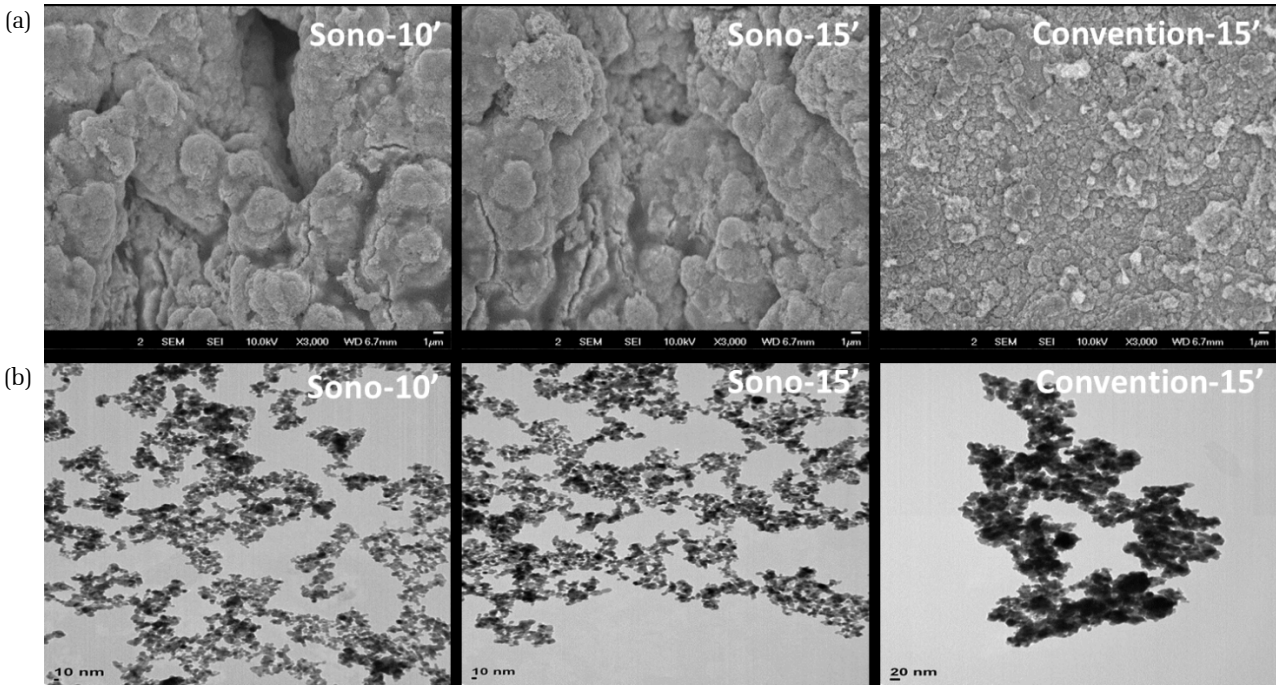

Fig. 2. SEM (a) and TEM (b) images of the RuO2 electrodes made by sonoelectrodeposition and conventional stirring electrodeposition. Sono-x′ and convention-x′: where x indicates the deposition time (min).

surface morphology of the RuO_2 electrode. Sonication removed all the hydrogen gas evolved from the surfaces, and it enhances the deposition process with well covered deposits (reference Supporting Information S1). The sonication wave makes the diffusion layer thinner and reduces the depletion of the electroactive surface near the substrate to form a hemisphere in the existing nucleus.

Fig. 2 (b) shows the difference in the crystal size of the RuO_2 nanoparticles produced by sonoelectrodeposition and conventional stirring electrodeposition. The water molecules in hydrous form are removed due to the annealing temperature. As a result, tiny sized RuO_2 crystals with 7-10 nm in diameter while that of the conventional method is 20-25 nm with high agglomerates. The nanoparticles made by the sonoelectrodeposition method are smaller in size and more uniform and have a finer distribution than the nanoparticles made by the conventional method.

From these observations, we postulated that the implosion of cavitation bubbles on the surfaces of the substrate, the acoustic streams enabling deagglomeration, and the activation of nucleation sites of RuO_2 all lead to a fine dispersion of RuO_2 nanoparticles on the surface. On the other hand,

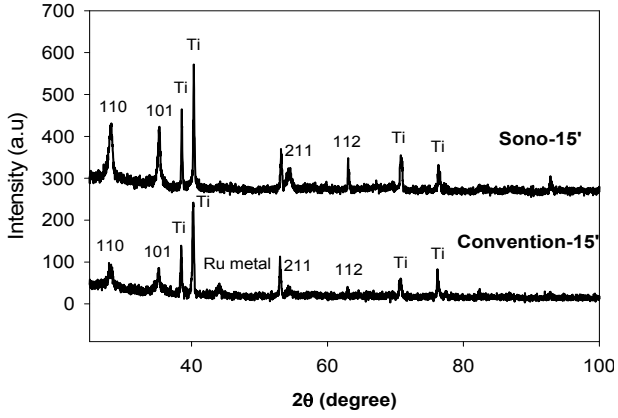

Fig. 3. XRD spectra of the RuO_2 electrodes made by sonoelectrodeposition and conventional stirring electrodeposition. Sono-x′ and convention-x′: where x indicates the deposition time (min).

there is no difference between the crystal size of the electrode made by sonoelectrodeposition after 10 and 15 min. It means that the sonoelectrodeposition time does not affect the crystal size of the RuO_2 electrodes (Pollet et al., 2011).

Fig. 3 shows the diffraction patterns of the RuO_2 electrodes made by sonoelectrodeposition and conventional stirring electrodeposition after 15 min. The typical peaks of the rutile

RuO_2 metal oxide easily detected.

The XRD spectra suggest that the oxide nanoparticles in all cases are fine and have a polycrystalline structure, which is desirable in terms of electrode stability. The peak for Ru metal is shown for the electrode made by conventional stirring electrodeposition, but it is not present for the electrode produced by the sonoelectrodeposition method. An electrode containing Ru metal is undesirable because it makes the electrode sensitive to corrosion during electrolysis. The Ru metal deposition is suppressed in sonoelectrochemical method, owing to the favored H2 generation in sonic ation.

Overall, the applied sonication has a significant positive influence on the resulting phase formation of RuO_2 electrodes.

3.3 Active surface area of RuO_2 electrode by sonoelectrodeposition method

Fig. 4 shows the extrapolated voltammetric charges (a) and cyclic voltammograms (b) from a set of RuO_2 electrodes made by sonoelectrodeposition and conventional stirring electrodeposition. As shown in Fig. 4 (a), the voltammetric charges (active surface areas) decrease with the increase in the scan rate. It indicates that it is difficult for the electrolyte to penetrate the inner surface of the electrode through structures such as micro pores, micro cracks, and grain boundaries.

The total and outer voltammetric charges for the 15 min sonoelectrodeposition electrode were 32.5 mC/cm^2 and 23.9 mC/cm^2 while the values for the conventional electrode were 22.2 mC/cm^2 and 14.2 mC/cm^2, respectively. The higher voltammetric charges of the electrodes due to the sonoelectrodeposition method can be attributed to the higher roughness factor, hemispheres, mushroom-like morphology, and decreased crystal sizes.

The total and outer voltammetric charges increased as the sonoelectrodeposition time was increased from 10 to 15 min. This result is due to the increased roughness factor and the amount of deposited RuO_2. The voltammetric charges of the electrodes due to sonoelectrodeposition after 10 min were also higher than those for the conventional electrode after 15 min. This result indicates that the outer active surface area of the RuO_2 electrode is more important than the total active surface area for the chlorine electrocatalytic activity (Burke et al., 1979; Trasatti et al., 1987; Chen et al., 2012[a]). The outer surface area is the main working part for chlorine evolution. The inner surface is blocked by adherent chlorine gas bubbles and becomes partially inactive (Chen et al., 2012[b]; Zeradjanina et al., 2012).

Fig. 4 (b) shows the cyclic voltammetry curves of sonoelectrodeposited RuO_2 electrodes. The current densities in the cyclic voltammetry are enhanced on the sonoelectrodeposited RuO_2 compared to the conventional one. It means that the electrodes made by sonoelectrodeposition have better

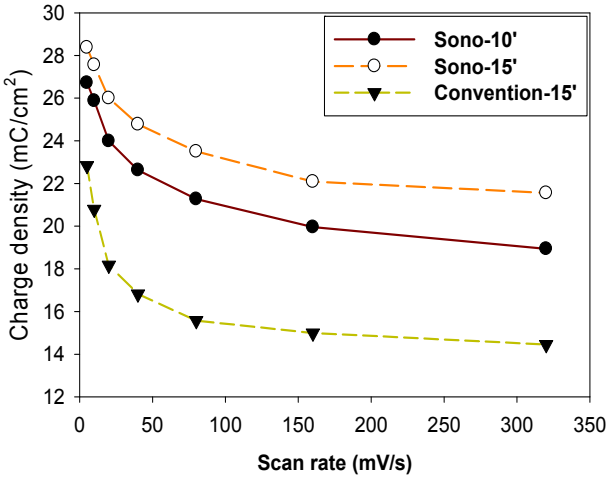

(a)

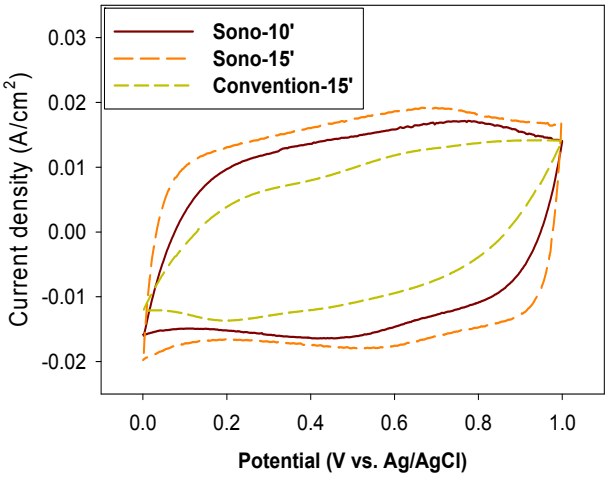

(b)

Fig. 4. Voltammetric charges (a) and cyclic voltammograms at 320 mV/s (b) in 0.5 M H_2SO_4 for RuO_2 electrodes made by sonoelectrodeposition and conventional stirring electrodeposition. Sono-x' and Convention-x': where x indicates the deposition time (min).

electrochemical properties. The rectangular shape of the cyclic voltammetry of the RuO_2 electrodes remains unchanged with the scan rate (Data not shown). The current densities extracted from the cyclic voltammograms in Fig. 4 (b) are very similar to the voltammetric charges shown in Fig. 4 (a) of these RuO_2 electrodes.

3.4 Sonoelectrodeposited amount of RuO_2

The electrodeposition experiments revealed the formation of black deposits on all the Ti substrates. The amount of RuO_2 nanoparticles deposited on the electrode surface can be measured by the film thickness or the increase in the weight of the electrode after and before deposition. An accurate measurement of the RuO_2 film thickness was not possible due to the rough morphology of the film. Therefore, the deposited weight (mg/cm2) of the RuO_2 film was measured instead of the thickness (Zhitomirsky et al., 1997).

Fig. 5 shows the weights of the RuO_2 films made by sonoelectrodeposition and conventional stirring electrodeposition for different deposition times. It was observed that the deposited weight was increased at longer sonoelectrodeposition time. However, the deposited weight did not significantly increase at the sonoelectrodeposition time above 15min, which might be caused by a lack of reactive species in the electrolyte.

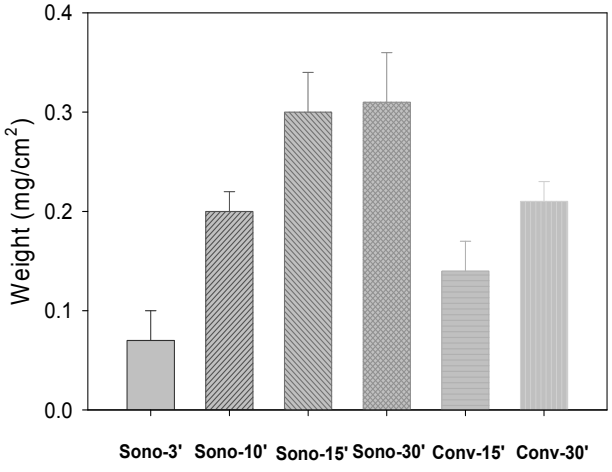

Fig. 5. Weights of RuO_2 deposits made by sonoelectrodeposition and conventional stirring electrodeposition for different deposition times with a constant current of 50 mA/cm^2. Sono-x′ and Convention-x′: where x indicates the deposition time (min).

The weight of the RuO_2 nanoparticles deposited by sonication for 10 min was 0.20 mg/cm^2. This value is close to the weight of the RuO_2 nanoparticles produced by the conventional stirring method for 15 min, which was 0.21 mg/cm^2. On the other hand, the weight of the RuO_2 nanoparticles deposited by sonication for 15 min was 0.30 mg/cm^2. It is higher than that for the conventional one. This result means that sonoelectrodeposition produces a larger amount of RuO_2 nanoparticles at the same amount of time. This might be caused by the removal of the H_2 bubbles, which enhances the mass transfer and the deposition process rates (Walker et al., 1997; Mallik et al., 2011; Pollet et al., 2011).

3.5 Accelerated stability test (AST) of RuO_2 electrode by sonoelectrodeposition method

Considering the industrial application of chlorine generating electrode, the stability should be considered. Therefore, the electrode lifetime was measured by stability test, which is defined by the time at which the potential of an electrode suddenly escalates under galvanostatic conditions in simultaneous oxygen and chlorine evolution reactions.

Fig. 6 shows the time dependencies of the electrode potential and the appropriate differential curves for the RuO_2

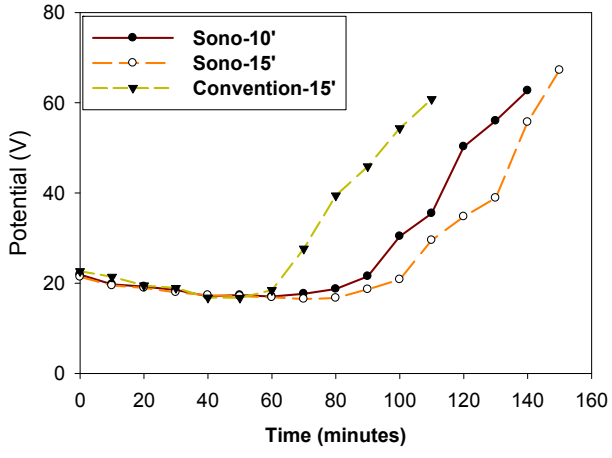

Fig. 6. The AST of the RuO_2 electrodes prepared by sonoelectrodeposition and conventional stirring electrodeposition. Sono-x′ and Convention-x′: x indicates the deposition time (min). (Experimental conditions: 0.5 M NaCl; pH 2; 25oC; 1 A/cm^2).

electrodes prepared by sonoelectrodeposition and conventional stirring electrodeposition. The potential seems to be slightly decreased over the initial period, and this result is related to the activation process. The life time of the RuO_2 electrodes made by the sonoelectrodeposition method (90 and 100 min) are longer than that for the electrode made by conventional stirring electrodeposition (60 min) under the same electrolysis condition.

The electrode stability increased as the sonoelectrodeposition time was increased from 10 to 15 min. This phenomenon can be explained by the mass coverage enhancement.

In general, the failure of the RuO_2 electrode is explained by three mechanisms, which are the growth of an insulating TiO2 layer at the coating (a substrate interface that becomes less doped with the catalytic oxide), the removal of the catalytic material by intense gas production, and the dissolution of Ru during long-term electrolysis (Ribeiro et al., 2004; Panic et al., 1999; Aromaa et al., 2006).

The higher stability of electrode with sonoelectrodeposition method might be ascribable to the morphology of the surface. The RuO_2 layer produced by this method is denser than the layer fabricated by conventional one, which makes lower penetration rate of electrolyte into Ti substrate. Thus, it enables the formation of a less non-conductive intermediate TiO_2 layer compared to the conventional electrode. Overall, the stability of the electrodes made by sonoelectrodeposition is higher than that made by conventional stirring electrodeposition.

4. Conclusions

This study reports on the sonoelectrodeposition of RuO_2 electrodes for chlorine generation. The electrode obtained by the sonoelectrodeposition method shows strong improvement in the electrocatalyst efficiency and stability for chlorine generation compared to the conventional stirring electrodeposition method.

Sonoelectrodeposition increases the external surface area of the RuO_2 electrode. In addition, this technique provides RuO_2 electrodes with broad hemispheres and mushroom-like and compact structures. It also produces a large amount of RuO_2 nanoparticles uniformly with a smaller size. Furthermore, the electrodes produced by the sonoelectrodeposition method do not contain undesirable Ru metal. Finally, the most important effect is the large increase of mass transfer to reduce the diffusion layer.

Acknowledgements

This research was supported by Korea Ministry of Environment as “Global Top Project (E617-00211-0608-0)" and a grant (code 17IFIP-B065893-05) from the Industrial Facilities & Infrastructure Research Program funded by the Ministry of Land, Infrastructure and Transport of Korea government.

References

A. Bard, L. Faulkner (2001). *Electrochemical methods - Fundamentals and applications*, 2nd edition, Wiley, New York pp. 200-217.

A. Mallik, B. Ray (2011). An analysis of the temperature-induced supersaturation effects on structure and properties of sono-electrodeposited copper thin films, Surf. Coat. Tech. 206 1947 – 1954.

A. J. Terezo, E. C. Pereira (2002). Preparation and characterization of Ti/RuO_2 anodes obtained by sol – gel and conventional routes, Mater. Lett. 53 339-345.

Apha, (2005). *Standard Methods for the Examination of Water and Wastewater*, 21st edition, American Public Health Association, Washington, DC. pp. 4-46.

A. Zeradjanina, F. Mantiab, J. Masaa, W. Schuhmann (2012). Utilization of the catalyst layer of dimensionally stable anodes — Interplay of morphology and active surface area, Electrochim. Acta. 82 408 – 414.

B. Park, C. Lokhande, H. Park, K. Jung, O. Joo, (2004). Cathodic electrodeposition of RuO_2 thin films from RuCl3 solution, Mater. Chem. Phys. 87 59 – 66.

B. Pollet, J. Hihn, T. Mason (2008). Sonoelectrodeposition (20 and 850 kHz) of copper in aqueous and deep eutectic solvents, Electrochim. Acta. 53 4248 – 4256.

B. Pollet, E. Valzer, Oliver J. Curnick (2011). Platinum sonoelectrodeposition on glassy carbon and gas diffusion layer electrodes, Int. J. Hydrogen Energy. 36 6248-6258.

C. Hu, H. Guo, K. Chang and C. Huang (2009). Anodic composite

deposition of RuO.·xH2O-TiO2 for electrochemical supercapacitors, Electrochem. Commun. 11 1631-1634.
C. Malmgren, A. K. Eriksson, A. Cornell, J. Backtrom, S. Eriksson, H. Olin (2010). Nanocrystallinity in RuO_2 coatings - Influence of precursor and preparation temperature, Thin Solid Films. 518 3615-3618.
E. Lecina, I. Urrutia, J. Diez, J. Morgiel, P. Indyka (2012). A comparative study of the effect of mechanical and ultrasound agitation on the properties of electrodeposited Ni/Al2O3 nanocomposite coatings, Surf. Coat. Tech. 206 2998 – 3005.
E. Tsuji, A. Imanishia, K. Fukuia, Y. Nakato (2011). Electrocatalytic activity of amorphous RuO_2 electrode for oxygen evolution in an aqueous solution, Electrochim. Acta. 56 2009 – 2016.
H. P. Klug, L. E. Alexander (1974). *X-ray Diffraction Procedures*, 2nd edition, Wiley, New York.
H. Zheng, M. An (2008). Electrodeposition of Zn – Ni – Al_2O_3 nanocomposite coatings under ultrasound conditions, J. Alloy. Comp. 459 548 – 552.
I. Zhitomirsky, L. Gal-Or (1997). Ruthenium oxide deposits prepared by cathodic electrosynthesis, Mater. Lett. 31 155-159.
J. Aromaa, O. Forse (2006). Evaluation of the electrochemical activity of a Ti – RuO_2 – TiO_2 permanent anode, Electrochim. Acta. 51 6104-6110.
J. Chou, Y. Chen, M. Yang, Y. Chen, C. Lai, H. Chiu, C. Lee, Y. Chueh and J. Gan (2013). RuO_2/MnO_2 core – shell nanorods for supercapacitors, J. Mater. Chem. A. 1 8753-8759.
J. Garcia, M. Esclapez, P. Bonete, Y. Hernandez, L. Garreton, V. Saez, (2010). Current topics on sonoelectrochemistry, Ultrasonics. 50 318-322.
J. Garcia, V. Saeza, M. Esclapeza, P. Bonetea, Y. Vargasb, L. Gaeteb (2010). Relevant developments and new insights on sonoelectrochemistry, Physics Proc. 3 117-124.
J. Garcia, V. Saez, J. Iniesta, V. Montiel, A. Aldaz, (2002). Electrodeposition of PbO2 on glassy carbon electrodes: influence of ultrasound power, Electrochem. Commun. 4 370-373.
J. Han, S. Lee, S. Kim, S. Han, C. Hwang, C. Dussarrat, and J. Gatineau, (2010). Growth of RuO_2 thin films by pulsed-chemical vapor deposition using RuO4 precursor and 5% H2 reduction gas, Chem. Mater. 22 5700-5706.
J. Jirkovsky, H. Hoffmannova, M. Klementova and P. Krtil (2006). Particle size dependence of the electrocatalytic activity of nanocrystalline RuO_2 electrodes, J. Electrochem. Soc. 153 111-118.
J. Jowa, H. Lee, H. Chena, M. Wu, T. Wei (2007). Anodic cathodic and cyclic voltammetric deposition of ruthenium oxides from aqueous RuCl3 solutions, Electrochim. Acta. 52 2625-2633.
J. Jeong, C. Kim, J. Yoon (2009). The effect of electrode material on the generation of oxidants and microbial inactivation in the electrochemical disinfection processes, Water Res. 43 895-901.
J. Ribeiro, M. Moats, A. Andrade (2008). Morphological and electrochemical investigation of RuO_2 – Ta_2O_5 oxide films prepared by the Pechini – Adams method, J. Appl. Electrochem. 38 767-775.
J. Ribeiro and A. Andrade (2004). Microstructure, morphology and electrochemical investigation characterization of RuO_2-Ta_2O_5 coated Titanium electrode, J. Electrochem. Soc. 151 106-112.
L. Burke and J. Mulcahy (1976). The formation and reduction of anodic films on electrodeposited ruthenium, J. Electroanal. Chem. 73 207-218.
L. D. Burke and J. F. O'Neill (1979). Some aspects of the chlorine evolution reaction at Ruthenium dioxides anodes, J. Electroanal. Chem. 101 341-349.
M. Hyde, R. Compton (2002). How ultrasound influences the electrodeposition of metals, J Electroanal. Chem. 531 19-24. (Hyde et al., 2002) [25]
M. Katerina, M. Marina; K. Petr (2009). Oxygen evolution on nanocrystalline RuO_2 and $Ru_{0.9}Ni_{0.1}O_2$ electrodes – DEMS approach to reaction mechanism determination. Electrochem. Commun. 11 1865-1868.
M. Macherzynskia, A. Kasuya (2013). Electrodeposition of uniformly distributed Ru and Ru – Pt nanoparticles onto n-type Si electrodes, Electrochim Acta. 95 288-294.
M. Metikos-Hukovic, R. Babic, F. Jovic, Z. Grubac (2006). Anodically formed oxide films and oxygen reduction on electrodeposited ruthenium in acid solution, Electrochim. Acta. 51 1157-1164.
M. Vukovic (1989). Oxygen evolution on an electrodeposited Ruthenium electrode in acid solution - the effect of thermal treatment, Electrochim. Acta. 34 287-291.
R. Burrows, D. Denton and J. Harrision (1978). Chlorine and oxygen evolution on various compositions of RuO_2/TiO_2 electrodes, Electrochim. Acta. 23 493-500.
R. Chen, T. Vinh, A. R. Zeradjanin, H. Natter, D. Teschner, J. Kintrup, A. Bulan, W. Schuhmann and R. Hempelmann (2012). Microstructural impact of anodic coatings on the electrochemical chlorine evolution reaction, Phys. Chem.

Chem. Phys. 14 7392-7399.

R. Chen, T. Vinh, N. Harald, J. Kintrup, A. Bulan, R. Hempelmann (2012). Wavelet analysis of chlorine bubble evolution on electrodes with different surface morphologies, Electrochem. Commun. 22 16-20.

R. Walker (1997). Ultrasound improves electrolytic recovery of metals, Ultrason. Sonochem. 4 39-43.

S. Ardizzone, G. Fregonara, S. Trasatti (1990). Inner and outer active surface of RuO_2 electrodes, Electrochim. Acta. 35 263-267.

S. Floate, M. Hyde, R. Compton (2002). Electrochemical and AFM studies of the electrodeposition of cobalt on glassy carbon: an analysis of the effect of ultrasound, J. Electroanal. Chem. 523 49-63.

S. Trasatti (1984). Electrocatalysis in the anodic evolution of oxygen and chlorine, Electrochim. Acta. 29 1503-1512.

S. Trasatti (1987). Progress in the understanding of the mechanism of chlorine evolution at oxide electrodes, Electrochim. Acta. 32 369-382.

T. L. Luu, C. Kim, J. Kim, S. Kim, J. Yoon (2015). The Effect of Preparation Parameters in Thermal Decomposition of Ruthenium Dioxide Electrodes on Chlorine Electro-Catalytic Activity, B. Kor. Chem. Soc. 36 1411-1417.

T. L. Luu, J. Kim, J. Yoon (2015). Physicochemical properties of RuO_2 and IrO_2 electrodes affecting chlorine evolutions, J. Ind. Eng. Chem. 21 400-404.

Y. Niu, J. Wei, Y. Yang, J. Hu, Z. Yu (2012). Influence of microstructure on the wear mechanism of multilayered Ni coating deposited by ultrasound-assisted electrodeposition, Surf. Coat. Tech. 210 21-27.

V. Panic, A. Dekanski, S. Milonjic, R. Atanasoski, B. Nikolic (1999). RuO_2 – TiO_2 coated titanium anodes obtained by the sol – gel procedure and their electrochemical behaviour in the chlorine evolution reaction, Colloids Surf. A. 157 269-274.

V. Panic, A. Dekanski, M. Stankovic, S. Milonjic, B. Nikoli (2005). On the deactivation mechanisms of RuO_2 – TiO_2/Ti anodes prepared by the sol – gel procedure, J. Electroanal. Chem. 579 67-76.

V. Saez, J. Garcia, J. Iniesta, A. Ferrer, A. Aldaz (2004). Electrodeposition of PbO_2 on glassy carbon electrodes: influence of ultrasound frequency, Electrochem. Commun. 6 757-761.

V. Srinivasan, P. Arora, P. Ramadass (2006). Report on the electrolytic industries for the year 2004, J. the Electrochem. Soc. 153 K1-K14.

V. Trieu, B. Schleya, H. Nattera, J. Kintrup, A. Bulan, R. Hempelmann (2012). RuO_2-based anodes with tailored surface morphology for improved chlorine electro-activity, Electrochim Acta. 78 188-194.

Y. Zheng, H. Ding, M. Zhang (2008). Hydrous – ruthenium – oxide thin film electrodes prepared by cathodic electrodeposition for supercapacitors, Thin Solid Films. 516 7381-7385.

SUPPORTING INFORMATION

Calculation the total and outer surface areas

The surface area was calculated from the voltammetric charge q obtained by integration of the voltammetric curve. In the low scan rate, the proton exchanges take place over the inner and outer surface. On the other hand, in the fast scan rate, the penetration of the protons into the inner surface is inhibited. Thus, only the outer surface contributes to the proton exchanges in the fast scan rate (Pollet et al., 2008). This phenomenon is due to the existence of less accessible surface regions like micro pores and micro cracks. Therefore, the inner and outer surface areas can be calculated by plotting and extrapolating the voltammetric charges according to infinitely low (0) and fast (∞) scan rates.

The following equations are used (Pollet et al., 2008):

$$q_{total} = q_{inner} + q_{outer} \quad (s1)$$

$$q(\nu) = q_{outer} + A(1/\sqrt{\nu}) \quad (s2)$$

$$1/q(\nu) = 1/q + B\sqrt{\nu} \quad (s3)$$

where: ν is the scan rate; $q(\nu)$ is the voltammetric charge at the scan rate ν; q_{total} is the voltammetric charge obtained at an infinitely low (0) scan rate; qouter is the voltammetric charge obtained at a high (∞) scan rate; q_{inner} is related to the voltammetric charge of the inner surfaces, and A, B are constants.

Fig. S1 shows the cathodic polarization curves of the $RuCl_3$ aqueous solution on the Ti substrates under the sonoelectrodeposition and the conventional stirring electrodeposition. The Ru^{3+} ions in the electrolyte solution were reduced at -0.2 V versus Ag/AgCl. The platform of limiting current and the diffusion current of the reduction of Ru^{3+} appears at 0 to -0.2 V versus Ag/AgCl. Hydrogen evolution occurs at -0.2 V versus Ag/AgCl. This result shows that reducing Ru^{3+} ions is only possible when H_2 and OH^- are generated on the electrode at -0.2 V versus Ag/AgCl. It is consistent with Zhitomirsky et al.'s results (Zhitomirsky et al., 1997). It suggests that the cathodic deposition is due to the reactions of Ru^{3+} ions on the electrode. Fig. S1 clearly shows that sonication affects the RuO_2 deposition process in the potential range studies. In the sonoelectrodepostion process, the cathodic currents shifts to the more negative region, and an increase in the pseudo limiting current densities are observed compared to the conventional stirring electrodepostion. It can be attributed by the highly efficient stirring, which causes the implosion of cavitation hydrogen bubbles (Hyde et al., 2002; Garcia et al., 2002; Saez et al., 2004; Pollet et al., 2011).

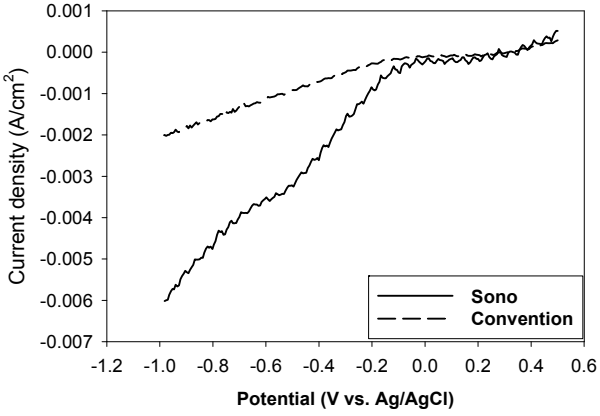

Fig. S1. Cathodic polarization curves of RuCl3 aqueous solution under sonoelectrodeposition and conventional stirring electrodeposition.